Atmos. Chem. Phys. Discuss., 10, 23657–23703, 2010
www.atmos-chem-phys-discuss.net/10/23657/2010/
doi:10.5194/acpd-10-23657-2010
© Author(s) 2010. CC Attribution 3.0 License.

Atmospheric Chemistry and Physics Discussions

This discussion paper is/has been under review for the journal Atmospheric Chemistry and Physics (ACP). Please refer to the corresponding final paper in ACP if available.

Air quality and emissions in the Yangtze River Delta, China

L. Li[1,2], C. H. Chen[2], C. Huang[2], Y. J. Wang[1], H. Y. Huang[2], J. M. Fu[1], J. S. Fu[3], D. G. Streets[4], G. F. Zhang[2], H. L. Wang[2], Y. R. Chen[2], and C. J. Jang[5]

[1]Institute of Environmental Pollution and Health, School of Environmental and Chemical Engineering, Shanghai University, Shanghai 200444, China
[2]Shanghai Academy of Environmental Sciences, Shanghai, 200233, China
[3]Department of Civil and Environmental Engineering, University of Tennessee, Knoxville, TN 37996, USA
[4]Decision and Information Sciences Division, Argonne National Laboratory, Argonne, IL 60439, USA
[5]Office of Air Quality Planning and Standards, US Environmental Protection Agency, Research Triangle Park, NC 27711, USA

Received: 23 August 2010 – Accepted: 27 September 2010 – Published: 12 October 2010

Correspondence to: C. H. Chen (chench@saes.sh.cn)

Published by Copernicus Publications on behalf of the European Geosciences Union.

Abstract

Regional trans-boundary air pollution has become an important issue in the field of air pollution modeling. This paper presents the results of the implementation of the MM5-CMAQ modeling system in the Yangtze River Delta (YRD) for the months of January and July of 2004. The meteorological parameters are obtained by using the MM5 model. A new regional emission inventory with spatial and temporal allocations based on local statistical data has been developed to provide input emissions data to the MM5-CMAQ modeling system. The pollutant concentrations obtained from the MM5-CMAQ modeling system have been compared with observational data from the national air pollution monitoring network. It is found that air quality in winter in the YRD is generally worse than in summer, due mainly to unfavorable meteorological dispersion conditions. In winter the pollution transport from Northern China to the YRD reinforces the pollution caused by large local emissions. The monthly average concentration of SO_2 in the YRD is $0.026 \pm 0.011\,mg\,m^{-3}$ in January and $0.017 \pm 0.009\,mg\,m^{-3}$ in July. Monthly average concentrations of NO_2 in the YRD in January and July are $0.021 \pm 0.009\,mg\,m^{-3}$, and $0.014 \pm 0.008\,mg\,m^{-3}$ respectively. Visibility is also a problem, with average deciview values of 26.4 ± 2.95 dcv in winter and 17.6 ± 3.3 dcv in summer. The ozone concentration in the downtown area of a city like Zhoushan can be very high, with the highest simulated value reaching 107 ppb. Our results show that ozone and haze have become extremely important issues in the regional air quality. Thus, regional air pollution control is urgently needed to improve air quality in the YRD.

1 Introduction

The Yangtze River Delta (YRD), characterized by high population density and well-developed industry, is one of the largest economic regions in China. With rapid economic development in recent years and high energy consumption, air pollutant

ACPD
10, 23657–23703, 2010

emissions are increasing steadily and the regional environment is deteriorating. Regional visibility is decreasing, ozone concentrations are increasing, and the ecological environment and health of the people are suffering. Many observational studies in the past (Chameides et al., 1999; Xu et al., 1999; Luo et al., 2000; Cheung and Wang, 2001; Wang et al., 2001a) showed that high ozone concentrations were beginning to appear in Eastern China. A project sponsored by China's National Natural Science Foundation, "The atmospheric physical and chemical process and its influence on ecosystem in the Yangtze River Delta," has conducted field surveys on air quality in the YRD, which indicate that the ozone concentration can be high in this region; the occurrence frequency of ozone concentrations higher than 0.16 mg m^{-3} reached 20% at some sites (Wang et al., 2003).

Fine particles and ozone are considered to be the most serious air pollutants of concern in China and the United States today, as well as in most metropolitan areas around the world (Streets et al., 2007). High ozone concentration at ground level increases the frequency of urban photochemical smog, accelerates the aging process of materials, threatens people's health, and causes serious damage to the ecological environment (Wang et al., 2001b). Thus, high ozone concentration has been a great concern of environmental scientists in China (Xu et al., 1999; Zhu and Xu, 1994). Fine particles not only cause worsening of regional visibility, but also seriously affect people's health. Fine particles and ozone are both formed through a serious of complex chemical reactions among primary pollutants in the air. The lifetime of ozone formed through VOC, NO_x, and SO_2 reactions is usually several days, which allows further meteorological processes to complicate the ozone formation and destruction processes (Finlayson-Pitts and Pitts, 1993). In addition, NO_x, VOC, SO_2, and NH_3 can generate particulate matter such as $(NH_4)_2SO_4$ and NH_4NO_3 through chemical reactions. Therefore, it is difficult to assess their environmental impacts solely by experimental studies and field observations (Tesche, 1983).

To assess air quality in the YRD, the US EPA's "One Atmosphere" model, the Community Multi-scale Air Quality Modeling System (CMAQ) (Dennis et al., 1996; Byun

ACPD
10, 23657–23703, 2010

et al., 1998; Byun and Ching, 1999), is used to simulate the chemical transport of air pollutants, driven by a new, comprehensive emission inventory. CMAQ is a chemical dispersion model representative of the third generation of air quality models and includes ozone, aerosols, acid deposition, visibility, air toxics, and mercury chemistry. Under a US EPA initiative, CMAQ has already been successfully transferred to the Asian situation and used to assess air quality in Beijing (An et al., 2007; Streets et al., 2007; Fu et al., 2008), the YRD (Li et al., 2008), the Pearl River Delta (PRD) (Wang et al., 2010), and across East Asia (Zhang et al., 2004, 2005, 2007; Fu et al., 2008; Lin et al., 2009). In this paper, the fifth-generation NCAR/Penn State Mesoscale Model (MM5) (Chen and Dudhia, 2001; Chen et al., 2005) is used to produce the necessary meteorological fields in 4-D data assimilation mode; CMAQ is used for the numerical simulation of air pollutant transport and transformation in the YRD.

2 Methodology

2.1 Input data

The methodology used in this paper is to simulate the atmospheric processes over the YRD domain with MM5-CMAQ and a new emission inventory, in order to obtain a dataset with air pollutant concentrations in time and space for the simulation periods, which can then be compared with monitored concentrations. The driving meteorological inputs are provided by MM5, and the meteorology-chemistry interface processor (MCIP) is used to transfer MM5 output into gridded meteorological field data as the input to CMAQ. The Carbon Bond-IV chemical mechanism (CB-IV) is used in the CMAQ model, which consists of 36 chemical species, 93 chemical reactions, and 11 photochemical reactions (Lamb, 1982). Geographic Information System (GIS) technology is applied in gridding the YRD regional emission inventory to the model domain.

ACPD
10, 23657–23703, 2010

2.2 Model domain and simulation episodes

The model domain is based on a Lambert conformal map projection, using a three-way nested mode with grid resolutions of 36 km (covering the whole of China), 12 km (covering Eastern China), and 4 km (covering the YRD region), as shown in Fig. 1. The large outer domain is centered at (110° E, 34° N). The YRD domain has 118×136 horizontal grid cells and includes 16 major cities, which are also shown in Fig. 1. Each "city" in the domain is a large administrative area that includes smaller cities, towns, and villages. Thus, the 16 cities together cover the majority of the YRD area. The pollution episodes chosen are 1–31 January 2004, and 1–31 July 2004, which represent winter and summer seasons, respectively. The initial conditions for each seasonal run are prepared by running the model five days ahead of each start date with clean initial conditions (IC). Sensitivity tests show that the influence of IC generally dissipates after about three days. The model employs 14 vertical layers of varying thickness with denser layers in the lower atmosphere to better resolve the mixing height.

2.3 Regional emission inventory

In this paper, a new emission inventory for the YRD was prepared, which consists of large point sources, industrial sources, mobile sources, residential sources, biomass burning, and biogenic sources. The basis of this inventory is a new compilation from local authorities of sources in the 16 major cities of the YRD domain.

Point sources in this inventory consist of power plants and large industrial combustion and process sources. The point source data are obtained from a national environmental statistical database provided by the Chinese Academy for Environmental Planning. Point sources are located at their exact lat/long coordinates within the domain.

Mobile sources mainly consist of on-road vehicle emissions in the 16 major cities. The vehicle volume data are collected from the statistical yearbooks of Jiangsu and Zhejiang Provinces and the Shanghai Municipality (Jiangsu Statistical Yearbook, 2005; Zhejiang Statistical Yearbook, 2005; Shanghai Statistical Yearbook, 2005).

ACPD
10, 23657–23703, 2010

Areas sources in this paper include fugitive emissions from industrial activity and residential fuel combustion. Residential emissions are calculated based on the consumption of coal, LPG, coal gas, and natural gas in 2004, as obtained from the statistical yearbooks of the 16 cities in the YRD.

Emission factor is an important element that influences the estimation of emission inventory. Supporting data on emission factors and activity data were assembled from related studies. Emission factors in this study are mainly referred to widely accepted studies or calculated based on related parameters. The SO_2 emissions from major pollutant sources are calculated based on fuel consumption and sulphur content. Results have been compared and verified with the environmental statistical data. Emission factors and fuel parameters are mainly from national literature, including "Environmental statistical mannual", "User's Guide on the Production and Emission Factors of Industrial Pollutants" and "Environmental protection data manual". Related data have been widely used in other studies (Streets et al., 2000; Kuang et al., 2001; Di et al., 2005). Emission factors of other pollutants like NO_x and CO are obtained through calculation or referred to related studies (Fang et al., 1985; Hu, 1990; Kato et al., 1992; Akimoto et al., 1994; MEP, 1996; Streets et al., 2000, 2001, 2003a, b). Emission factors of VOC, NH_3, PM_{10} and $PM_{2.5}$ are mainly obtained through literature survey (Kato et al., 1992; Akimoto et al., 1994; Streets et al., 2000, 2001, 2003a, b; USEPA, 2006). Currently we are lack of measurement data to verify those emission factors, which could likely be taken into consideration in the future studies.

The newly calculated emissions for the 16 cities in the YRD are then inserted into the regional East Asian emission inventory provided by TRACE-P (Streets et al., 2003a,b; Fu et al., 2008), which provides emissions data for the remaining parts of the domain. The TRACE-P emission inventory has been described and demonstrated to be reliable for China in previous studies (Streets et al., 2003a,b; Carmichael et al., 2003).

ACPD
10, 23657–23703, 2010

3 Results and discussion

3.1 Regional emission inventory for the YRD

3.1.1 Point sources

There were 378 power plants in the 16 cities of the YRD in 2004. In addition, there were 9793 major industrial sources, among which there were 4381 in Jiangsu Province (44.7%), 3864 in Zhejiang Province (39.5%), and 1548 in Shanghai Municipality (15.8%). Figure 2 shows the distribution of these point sources in the YRD. This is the first time that a comprehensive allocation of emissions to major point sources in the YRD has been developed. In 2004, the emissions of SO_2, NO_x, CO, PM_{10}, $PM_{2.5}$, and VOC in the power-plant sector were 1381, 727, 157, 660, 346, and 7 Gg, respectively. Emissions from power plants in Jiangsu Province are the highest, representing shares of 48%, 48%, 53%, 60%, 60%, and 51%, respectively, in the power-plant emissions of the pollutants listed above. Although there are only 19 power plants in Shanghai Municipality, they tend to be large ones, with shares of 18%, 19%, 20%, 7%, 7%, and 20%, respectively.

Emissions of SO_2, NO_x, CO, PM_{10}, $PM_{2.5}$, and VOC from fuel combustion in the industrial sector are 311, 168, 38, 341, 140, and 2 Gg, respectively. The emissions from fuel combustion in industry are highest in Jiangsu Province with shares of 54%, 38%, 34%, 49%, 50%, and 31%, respectively. Process emissions of SO_2, NO_x, CO, PM_{10}, $PM_{2.5}$, VOC, and NH_3 from the industrial sector are 63, 21, 378, 603, 335, 284, and 31 Gg, respectively. Jiangsu Province is again the highest emitter, with shares of 58%, 43%, 58%, 41%, 42%, 46%, and 52%, respectively.

3.1.2 Mobile sources

Figure 3 shows the vehicle stocks in each of the major cities of the YRD in 2004. There were 3 286 000 cars in the 16 cities, among which Jiangsu Province contains 1 270 000,

ACPD
10, 23657–23703, 2010

Zhejiang Province contains 1 141 000, and Shanghai contains 878 000. Among all the 16 cities, Shanghai, Hangzhou, Suzhou, Ningbo, and Nanjing contain the largest vehicle stocks, with shares of 26%, 12%, 11%, 8%, and 8%, respectively. In addition, there were 9 798 000 motorcycles and 7 266 000 light-duty motorcycles in the major cities of the YRD in 2004. Jiangsu, Zhejiang, and Shanghai own 59%, 40%, and 1% of the total motorcycles and 12%, 74%, and 14% of the light-duty motorcycles, respectively.

The compositions of the vehicle fleets are very different between Shanghai Municipality and the two neighboring provinces. Figure 4 shows the vehicle stocks by category in the two provinces and Shanghai. In Shanghai, light-duty cars represent 30% of total vehicles; while motorcycles (including light-duty motorcycles) are a major vehicle category in Jiangsu and Zhejiang Provinces, with shares of 80% and 73%, respectively.

Based on these vehicle stock data and local emission factors, the mobile source emissions of CO, VOC, NO_x, PM_{10}, and SO_2 in the YRD in 2004 were estimated to be 2302, 446, 358, 62, and 11 Gg, respectively. Regional shares for each of the species were for Jiangsu Province 49%, 50%, 46%, 50%, and 44%, for Zhejiang Province 28%, 30%, 29%, 29%, and 29%, and for Shanghai 24%, 20%, 25%, 22%, and 28%. Since Shanghai is a megacity with large numbers of vehicles, it has a larger share of mobile-source emissions than stationary sources. Since the vehicle mileage of heavy-duty trucks in Jiangsu Province is very high, the NO_x and PM_{10} emissions in the cities of Jiangsu Province are high. In addition, the large stocks of motorcycles and light-duty motorcycles are major sources of CO and VOC emissions in the YRD.

3.1.3 Area sources

Emissions from residential fuel combustion are calculated directly from fuel-use data for each of the cities in the region. Table 1 shows the residential fuel consumption in the cities of the YRD in 2004, as well as the populations of the cities. Though coal and LPG are used extensively in Jiangsu Province and Zhejiang Province, gas – both coal gas and natural gas – is preferred in Shanghai.

ACPD
10, 23657–23703, 2010

Fugitive emissions from industrial activity are calculated based on the consumption of coal and fuel oil in the YRD after energy consumption in the power plant, industry, transportation, and residential sectors is eliminated. Results show that in 2004, the emissions of SO_2, NO_x, CO, PM_{10}, $PM_{2.5}$, and VOC from residential fuel combustion were 16.4, 8.6, 17.6, 2.9, 1.7, and 1.0 Gg, respectively. Emissions of SO_2, NO_x, CO, PM_{10}, $PM_{2.5}$, VOC, and NH_3 from fugitive emissions of industry were 288, 114, 257, 28, 19, 26 and 1 Gg, respectively.

3.2 Model performance

3.2.1 Observational sites used to compare against MM5-CMAQ model results

In this paper we use selected hourly concentration data for SO_2, NO_2, PM_{10}, and O_3 measured during the periods 11–20 January 2004, and 11–20 July 2004, at each of the 43 national observational sites located in the YRD to assess the performance of the model. The locations of the measurement sites are shown in Fig. 5.

3.2.2 MM5 performance

A subjective test was performed on the 10-meter-height wind flow patterns as the first step in model performance evaluation. Figure 6 shows both NCEP observational data at 20:00 LT on 1 January 2004, and the model result. Comparison between the two figures shows that MM5 correctly reproduces the major patterns of the observed wind flow and that wind speed is within acceptable error limits.

A more objective test of MM5 performance was carried out using the method put forward by Keyser and Anthes (Pielke, 1990). Equations (1) to (4) were used to evaluate the MM5 results:

$$E = \left[\frac{1}{N}\sum(\Phi_i - \Phi_{\text{iobs}})^2\right]^{1/2} \quad (1)$$

ACPD
10, 23657–23703, 2010

$$E_{UB} = \left\{\frac{1}{N}\sum[(\Phi_i - \Phi_{iobs}) - \frac{1}{N}\sum(\Phi_i - \Phi_{iobs})]^2\right\}^{1/2}$$

$$= \left\{\frac{1}{N}\sum[(\Phi_i - \Phi_0) - (\Phi_{iobs} - \Phi_{obs})]^2\right\}^{1/2} \quad (2)$$

$$\sigma = \left[\frac{1}{N}\sum(\Phi_i - \Phi_0)^2\right]^{1/2} \quad (3)$$

$$\sigma_{obs} = \left[\frac{1}{N}\sum(\Phi_{iobs} - \Phi_{obs})^2\right]^{1/2} \quad (4)$$

where, E is the mean square error, which shows the deviation between prediction and observational data;
E_{UB} is the mean square without error, showing dispersion between prediction error and mean error;
Φ_i is the prediction value in a single grid and Φ_{iobs} is the observed value;
Φ_0 and Φ_{obs} are the mean values of Φ_i and Φ_{iobs}, respectively;
N is the number of observational sites; and
σ and σ_{obs} are the standard errors of predictions and observations.

When the following conditions are fulfilled, the model reliability is confirmed:

(1) $\sigma \approx \sigma_{obs}$,

(2) $E < \sigma_{obs}$,

(3) $E_{UB} < \sigma_{obs}$.

In order to compare the model results with observed NCEP data, the differences in spatial resolution must be addressed. The resolution of the outer model grid is 36 km, whereas the resolution of the NCEP data is 111 km. The two data sets were compared for regions that are almost coincident: 28° N–35° N/118° E–123° E (NCEP data)

ACPD
10, 23657–23703, 2010

and 28.12° N–34.94° N/118.08° E–122.95° E (modeled data). Coefficients between the predicted and observed values were calculated for selected time periods in January and July, 2004. Table 2 shows statistical analysis of horizontal (U) and vertical (V) wind speed at 10 m height. Coefficients equal to or greater than 0.5 are considered reliable. Table 2 demonstrates that the MM5 performance is reliable. Figure 7 shows comparisons of the temporal variation of wind speed between model and NCEP data in one specific grid cell at 08:00 LT and 20:00 LT on each day of January and July of 2004. Results show that MM5 performs well at reproducing the observed situation.

3.2.3 CMAQ performance test results and analysis

Sulfur dioxide

Figure 8 shows a comparison between the observed and modeled SO_2 concentrations at the Nantong, Shanghai, and Hangzhou observational sites during 11–20 January and 11–20 July 2004. It is to be expected that CMAQ would perform relatively well at predicting SO_2 concentrations, because the emission inventory is most reliable for SO_2 emissions that do not involve large contributions from small, dispersed sources, and because the chemistry and transport of SO_2 has been extensively studied for many years. Results show that CMAQ reproduces the variation trends of this pollutant well at each site. This provides additional confidence in the emission inventory of SO_2 in the YRD in 2004 and confirms that the meteorological fields used and the assumptions made in the CMAQ model reflect the true SO_2 pollution situation in the YRD.

Nitrogen dioxide

Figure 9 shows the comparison between model results and observational data of NO_2 hourly concentrations at Nanjing, Shanghai, and Hangzhou monitoring sites during 11–20 January and 11–20 July 2004. Results show that CMAQ can reproduce the variation trends of the pollutant concentrations. The modeling results for Nanjing, Shanghai, and

ACPD
10, 23657–23703, 2010

Hangzhou are good and reflect the actual NO_2 pollution status in these cities. However, the NO_2 simulation results are not as good as for SO_2; this is because the NO_x sources are smaller and more distributed than SO_2. The NO_x emission sources include not only power plants, industrial boilers and kilns, but also the emissions from mobile sources and residential combustion. Therefore, their magnitude and spatial distribution are more uncertain. In addition, of course, the local chemistry of NO_x emissions conversion is more complex than that of primary SO_2 emissions. NO_x conversion may be affected by possible underestimation of VOC emissions; some fugitive VOC emissions such as painting and evaporative emissions at gasoline refilling stations are not included in the inventory. In addition, the estimation of NH_3 emissions in the 16 city areas may be lower than in reality, because NH_3 emissions from fertilizer usage and livestock breeding in rural areas can be significant but are not included in the inventory. Thus, the transformation from NO_x, VOC, and NH_3 to particles may be underestimated in the model, which causes uncertainty in the NO_2 modeling result.

Particulate matter (PM)

Influenced heavily by meteorological conditions, PM_{10} concentrations are quite significant in winter time. Figure 10 shows a comparison between model results and observational data of PM_{10} hourly concentrations at Nantong, Ningbo, Jiaxing, and Huzhou monitoring sites during 11–20 January and 11–20 July 2004. Results show that CMAQ can reflect the trends of PM_{10} in January, while in July the model tends to underestimate the PM_{10} concentrations. There are four possible reasons. First, the PM_{10} emission inventory for the region may be underestimated, since fugitive dust emissions from construction sites, road transportation, coal stockpiles, etc., are not included. Second, since NH_3 emissions from rural areas are not considered, the transformation from NO_x and NH_3 to particles is weaker than expected. Third, VOC emissions in this study may be underestimated since there are some source types that are not included in the emission inventory; thus, fine particles formed through complex chemical reactions involving NO_x, VOC, etc., may be underestimated. Last but not least, on the occasions

ACPD
10, 23657–23703, 2010

of high pollution episodes, particularly in winter, the dominant wind is from a northerly direction and carries pollutants from north to south and affects the regional air quality in the YRD. In such cases, especially when there are dust storms in Northern China, our local emission inventory and even the regional TRACE-P inventory may not include all PM emissions and the modeled results may be lower than the observed ones.

Ozone

Hourly O_3 concentration data were only collected for Nanjing in January 2004 and for Shanghai in July 2004. Therefore, the observational data that are available for model testing are limited. Figure 11 shows the comparisons between model results and available monitoring data for hourly O_3 concentrations in January and July. Results show that CMAQ can reflect the variation trends of the pollutant. Specifically, the model gives reliable results for the summer case. Figure 11 shows that the model reproduces the daily change of O_3 concentration. With increase of solar radiation early in the day, the O_3 concentration rises; while in the afternoon, with decrease of radiation, the O_3 concentration gradually declines. The ozone concentration is influenced by emissions of precursors like NO_x and VOC, VOC speciation, and the temporal profiles of the emissions. The VOC speciation is compiled based on a literature survey (Streets et al., 2003a), but is known to be based largely on western sources, rather than Chinese sources, most of which have never been measured. The modeled O_3 concentration at midnight is not as low as expected, which is due to the PBL height simulation by MM5. In this paper, the MRF parameters are adopted in MM5 modeling, which usually gives high PBL height in daytime and low PBL at night. This systematic error tends to result in underestimation of ozone concentrations in the daytime and overestimation at nighttime.

ACPD
10, 23657–23703, 2010

Factor 2 analyses

Factor 2 analysis is one of the methods commonly used to check whether the air quality model results are acceptable. Factor 2 calculates the percentage of the ratios of model value to observational value that lie between 0.5 and 2. The calculation formula is shown in Eq. (5):

$$R = \frac{N_{[1/2,2]}}{N_t} \tag{5}$$

where, R is the percentage of the ratio between 0.5 and 2;
$N_{[1/2,2]}$ is the number of the ratio between 0.5 and 2; and
N_t is the total number of comparison points.

The larger the R value, the better the model performs. R=100% means the model performance is perfect. Figure 12 shows the factor 2 analysis results for SO_2, NO_2, and PM_{10}. Results show that in January, 59%, 80%, and 51% of the ratios between model and observational data for SO_2, NO_2, and PM_{10}, respectively, are within the factor 2 ranges. For the month of July, 75%, 81%, and 73% of the ratios of SO_2, NO_2, and PM_{10}, respectively, are within the factor 2 range. Generally speaking, the model performs quite well in the prediction of SO_2, NO_2, and PM_{10}. However, for ozone, there are only 32% and 50% of the results in winter and summer, respectively, within the factor 2 range. As shown in the figure, there are many points with modeled data higher than the observed ones, which is possibly due to the low PBL height at nighttime obtained by MM5, as mentioned above.

3.2.4 Statistical analysis of the performance results

To further study the model capability and applicability in the model domain, the following statistical measures were applied: normalized bias, index of agreement, correlation coefficient, and factor of two. The normalized bias is calculated by Eq. (6):

ACPD
10, 23657–23703, 2010

$$\text{Bias} = \frac{1}{N}\sum_{i=1}^{N}\frac{p_i - o_i}{o_i} \quad (6)$$

where p_i represents the predicted data and o_i represents the observational data. N means the number of data points. A normalized bias less than ±15% is suggested by EPA as indicative of acceptable ozone model performance.

The index of agreement is calculated by Eq. (7):

$$I = 1 - \frac{\sum_{i=1}^{N}(p_i - o_i)^2}{\sum_{i=1}^{N}\left(\left|p_i - \overline{o}\right| + \left|oi - \overline{o}\right|\right)^2} \quad (7)$$

where $\overline{o}$ denotes the average observed ozone concentration and a value of 1 indicates perfect agreement between predicted and observed values.

The statistical results comparing predicted values and observation data are given in Table 3. Table 3 shows that the correlation coefficients between prediction and observational data are mostly >0.5. The indexes of agreement of SO_2, NO_2, and PM_{10} are 0.55, 0.79, and 0.45, respectively, in January; and 0.79, 0.75, 0.53 in July. The CMAQ model overpredicts SO_2 and NO_2 concentrations by about 13–25% and 22–29%, while it underpredicts PM_{10} by about 24% in January and overpredicts by about 25% in July. The model performance for summer is better than winter. The reason for overprediction of SO_2, NO_2, and underestimation of PM_{10} is possibly due to underestimation of NH_3 emissions. The secondary transformation process is underestimated as a result. In winter, the meteorological dispersion conditions in the YRD are not good, generally with low wind speed, low precipitation, and frequent inversions; such complex meteorological conditions are not well simulated by meteorological models. For example, the wind speed obtained by MM5 is often overestimated and then the model results for winter are not as good as for summer. Although there are some biases in the model performance, these biases are generally within acceptable ranges.

ACPD
10, 23657–23703, 2010

4 Regional air quality model results and discussion

4.1 Ozone

Figure 13 shows the monthly average concentrations of O_3 and NO_2 in the 16 cities of the YRD. In January, the monthly average concentration of O_3 is 0.052 ±0.011 mg m^{-3}, and 0.054 ±0.008 mg m^{-3} in July. Due to the strong oxidation of O_3, the area with large NO_x emissions also shows high NO_2 concentrations; the NO_2 subsequently reacts with O_3 and reduces the O_3 concentration. The relationship between the O_3 and NO_2 concentrations shows that the two pollutants are negatively correlated, with a correlation coefficients of −0.85, as shown in Fig. 14. This result agrees with the observational work of Wang et al. (2001a).

To illustrate the formation and dissipation of ozone, Fig. 15 presents the variation of hourly O_3 concentration on 5 July 2004. The spatial distribution of ground-level O_3, influenced by meteorological conditions, varies with time. After the sun rises, the O_3 concentration gradually increases. As time goes by, the high O_3 concentration, influenced by southeasterly winds, gradually diffuses from Zhoushan, Ningbo, and Shaoxing to the north and west parts of the region. By 13:00–15:00 LT, the high hourly O_3 concentration covers the cities of Shaoxing, Hangzhou, Huzhou, and Jiaxing. The highest hourly concentration of O_3 on 5 July reached 107 ppb in the grid cell (112, 25) (Zhoushan City) at 13:00 LT. In Shanghai city, the figure shows obvious differences of O_3 concentrations at different locations. The ozone concentration in the urban area is lower than that in the rural area, because the emission characteristics in different regions of the city vary significantly. This result agrees with the work of Geng et al. (2008), who found that the O_3 concentration is highest in the rural area that has low emissions of O_3 precursors. In contrast, the O_3 concentration in the urban area is low due to the O_3 suppression processes caused by urban emissions.

ACPD
10, 23657–23703, 2010

4.2 Visibility

Visibility in the YRD is often poor, as can be readily observed by residents and visitors. This paper applies the concept of deciview (dcv) to reflect the visibility status. This indicator is calculated based on the extinction coefficient shown in Eq. (8).

$$dV = 10\ln(\beta/0.01) \quad (8)$$

where dV means deciview, and β represents the extinction coefficient.

In the United States, dcv is usually divided into five classes to reflect the subjective visibility levels, as shown in Table 4. Figure 16 shows the monthly average dcv values for the 16 major YRD cities obtained from the MM5-CMAQ model. The results show that the dcv values of the various cities in winter are >20, with an average value of 26.4±2.95 dcv, while the average visibility in summer is 17.6±3.3 dcv. As CMAQ underestimates PM_{10} concentrations about 24% in January and overpredicts about 26% in July, it can be inferred that $PM_{2.5}$ concentrations may also be underesimated in January and overpredicted in July, which indicates that the visibility should be worse than the simulation in January and better than modeling results in July. This shows that the visibility in the YRD in winter is quite bad, while it is relatively better in summer. This is mainly because the dominant wind in summer is southeast, which is from the East China Sea. Clean marine air makes the air quality good in summer. However, in winter, the meteorological conditions are not good for air pollutants to disperse. The wind speed is low, precipitation is rare, and frequency of inversion is high, which causes the air pollutants to accumulate readily. Thus the visibility in winter is relatively bad. Related studies show that visibility is strongly negatively correlated with $PM_{2.5}$, with a correlation coefficient of −0.68 (Huang et al., 2009). It is clear that $PM_{2.5}$ concentrations in the YRD cities are worse in the winter than in the summer, leading to poor visibility in winter. This result agrees with the work of Wang et al. (2006) and Ye et al. (2003), who found that the seasonal variation of ion and $PM_{2.5}$ concentrations was significant, with the highest concentrations observed in winter and spring and the lowest in summer and autumn.

ACPD
10, 23657–23703, 2010

Figure 17 shows the daily average dcv values for 10 January and 10 July 2004. Comparing the two images, we can see quite clearly that the visibility in winter is much worse than summer. In winter, the visibility in the center of the YRD – Hangzhou, Huzhou, Nanjing, Wuxi, and Changzhou cities – can be quite bad. While in the more eastern and southern areas, like Shanghai and Zhoushan, it is relatively better.

4.3 Other pollutants

Figure 18 shows the monthly average concentrations of SO_2 in the 16 cities of the YRD. In January, the monthly average concentration of SO_2 is $0.035 \pm 0.015\,mg\,m^{-3}$, and $0.019 \pm 0.010\,mg\,m^{-3}$ in July. As CMAQ overpredicts SO_2 concentrations by about 25% in January and 13% in July, we may anticipate that the real monthly average concentrations of SO_2 in the YRD in January and July are $0.026 \pm 0.011\,mg\,m^{-3}$, and $0.017 \pm 0.009\,mg\,m^{-3}$, respectively. Due to the air pollution transport from northern China to the YRD, together with the high local emissions, the regional SO_2 pollution in winter is worse than in summer. The pollution centers include Shanghai, Suzhou, Jiaxing, and Ningbo. In summer, due to inflow of clean air from the sea to the southeast, the SO_2 concentrations in cities are lower. The SO_2 concentrations in southern cities are obviously better than in the northern ones.

Figure 19 shows the monthly average concentrations of NO_2 in the 16 cities of the YRD. In January, the monthly average concentration of NO_2 is $0.029 \pm 0.012\,mg/m^3$, and $0.018 \pm 0.010\,mg/m^3$ in July. As CMAQ overpredicts NO_2 concentrations by about 29% in January and 22% in July, we may anticipate that the real monthly average concentrations of NO_2 in the YRD in January and July are $0.021 \pm 0.009\,mg/m^3$, and $0.014 \pm 0.008\,mg/m^3$, respectively. Similar to SO_2, Shanghai is also the high pollution center of NO_2. Comparisons between winter and summer show that, although there is clean air inflow from the sea in summer, the difference between seasons are not so obvious as for SO_2, which is due to the vehicle emissions in cities. In addition, in summer, due to use of air conditioners in the cars, the emissions are relatively higher

ACPD
10, 23657–23703, 2010

than in winter. This result is consistent with the work of Uno et al. (2007), who found that the seasonal variation of NO_2 over East Asia shows a summer (July–August) minimum and a winter (December) maximum. The result is also similar to that of Wang et al. (2009), who presented a seasonal variation in NO2 columns in the YRD region that showed higher NO_2 in winter due to the longer lifetime of NO_2 and greater NO_x emissions in the region.

5 Conclusions

This paper applies the MM5-CMAQ modeling system for the first time to the study of regional air pollution in the YRD. Model performance studies show that the system can reliably reproduce the air pollution situation in the region. Model performance results indicate that the correlation coefficients between prediction and observational data are greater than 0.5. The indexes of agreement for SO_2, NO_2, and PM_{10} are 0.55–0.79, 0.75–0.79, and 0.45–0.53, respectively. The CMAQ model tends to overpredict SO_2 and NO_2 concentrations by about 13–25% and 22–29%, while it underpredicts PM_{10} by about 24% in January and overpredicts by about 25% in July. The model performance for summer is better than winter. The model performance assessments show that the model results are acceptable for this application.

Observational data show that the ozone concentrations in summer are quite high, while the visibility in winter is bad. Model results show that the highest hourly concentration of O_3 on 5 July reached 107 ppb, which appeared at 13:00 LT in Zhoushan City, slightly lower than the observed value. The results also show that the deciview values for various cities in winter are >20, with an average value of 26.4±2.95 dcv, while the average visibility in summer is 17.6±3.3 dcv. The monthly average concentrations of NO_2 in the YRD in January and July are $0.021 \pm 0.009\,mg\,m^{-3}$, and $0.014 \pm 0.008\,mg\,m^{-3}$, respectively. Monthly average concentration of SO_2 in January is $0.026 \pm 0.011\,mg\,m^{-3}$, and $0.017 \pm 0.009\,mg\,m^{-3}$ in July. Due to pollutant transport from Northern China to the YRD, the unfavorable meteorological dispersion conditions,

ACPD
10, 23657–23703, 2010

and the high local emissions, the regional SO_2 pollution in winter is worse than in summer. Clearly, elevated O_3 episodes are occurring in the YRD, and regional haze is becoming more obvious. These results confirm the conclusions reached by Chan and Yao (2008), who reviewed the current state of understanding of the air pollution problems in Shanghai. However, details of these episodes, such as the frequency, the weather conditions, and the temporal and spatial variations of O_3 and haze, can vary significantly with geographical location within the region.

Currently, ozone and haze have become extremely important issues in regional air quality. The YRD is presently undergoing tremendous economic growth, and the threat of high regional pollutant emissions and high pollution is very real. In this point, we recommend that integrated measures be taken together in all the cities to improve the regional air pollution situation in the YRD.

Acknowledgements. The authors would like to thank Chinese Academy for Environmental Planning for supporting the "Regional Air Pollution Transportation" project and providing the basic emission related data. We would like to thank US EPA for providing the CMAQ model code, full model documentation, and assistance with model set-up and running. We also appreciate the suggestions made by anonymous reviewers that helped greatly to improve this paper.

References

Akimoto, H. and Natrita, H.: Distribution of SO_2, NO_x and CO_2 emissions from fuel combustion and industrial activities in Asia with $1^\circ \times 1^\circ$ resolution, Atmos. Environ., 28, 213–225, 1994.

An, X., Zhu, T., Wang, Z., Li, C., and Wang, Y.: A modeling analysis of a heavy air pollution episode occurred in Beijing, Atmos. Chem. Phys., 7, 3103–3114, doi:10.5194/acp-7-3103-2007, 2007.

Byun, D. W. and Ching, J. K. S.: Science algorithms of the EPA Models-3 Community Multiscale Air Quality (CMAQ) modeling system, US Environmental Protection Agency Report EPA/600/R-99/030, Research Triangle Park, NC, 1999.

Byun, D. W., Ching, J. K. S., Novak, J., and Young, J.: Development and implementation of the

ACPD

10, 23657–23703, 2010

EPA's Models-3 initial operating version: Community Multi-scale Air Quality (CMAQ) model, Plenum Publishing Coorp, New York, USA, 1998.
Carmichael, G. R., Tang, Y., Kurata, G., Uno, I., Streets, D. G., Thongboonchoo, N., Woo, J.-H., Guttikunda, S., White, A., Wang, T., Blake, D. R., Atlas, E., Fried, A., Potter, B., Avery, M. A., Sachse, G. W., Sandholm, S. T., Kondo, Y., Talbot, R. W., Bandy, A., Thornton, D., and Clarke, A. D.: Evaluating regional emission estimates using the TRACE-P observations, J. Geophys. Res., 108, 8810, doi:10.1029/2002JD003116, 2003.
Chameides, W. L., Li., X., Tang, X., Zhou, X., Chao, L., Kiang, C. S., St. John., J., Saylor, R. D., Liu, S. C., Lam, K. S., Wang, T., and Giorgi, F.: Is ozone pollution affecting crop yields in China?, Geophys. Res. Lett., 26, 867–870, 1999.
Chan, C. K. and Yao, X. H.: Air pollution in mega cities in China, Atmos. Environ., 42, 1–42, 2008.
Chen, F. and Dudhia, J.: Coupling and advanced land-surface/hydrology model with the Penn State/NCAR MM5 modeling system, part I: model implementation and sensitivity, Mon. Weather Rev., 129, 569–585, 2001.
Chen, S. J., Tong, J. C., Kazuhiko, K. B, and Zhu, J. G.: Influences of the meteorological factors on the ozone concentration near the ground, J. Central China Normal University (Nat. Sci.), 39, 273–277, 2005 (in Chinese).
Cheung, V. T. F. and Wang, T.: Observational study of ozone pollution at a rural site in the Yangtze River Delta of China, Atmos. Environ., 35, 4947–4958, 2001.
Dennis, R. L., Byun, D. W., Novak, J. H., Galluppi, K. J., Coats, C. J., and Vouk, M. A.: The next generation of integrated air quality modeling: EPA's Models-3, Atmos. Environ., 30, 1925–1938, 1996.
Di, X. H., Nie, Z. R., and Zuo, T. Y.: Life cycle emission inventories for the fuels consumed by thermal power in China, China Environmental Science, 25, 632–635, 2005 (in Chinese).
Fang, P. X., Jiang, X., and Xi, Y. F.: Environmental Statistics Mannual, Sichuan Science and Technology Press, Chengdu, China, 1985 (in Chinese).
Finlayson-Pitts, B. J. and Pitts, J. N.: Atmospheric chemistry of tropospheric ozone formation: scientific and regulatory implications, J. Air Waste Manage., 43, 1091–1100, 1993.
Fu, J. S., Streets, D. G., Jang, C. J., Hao, J., He, K., Wang, L., and Zhang, Q.: Modeling regional/urban ozone and particulate matter in Beijing, China, J. Air Waste Manage., 59, 37–44, 2009.
Fu, J. S., Jang, C. J., Streets, D. G., Li, Z., Kwok, R., Park, R., and Han, Z.: MICS-Asia II:

ACPD
10, 23657–23703, 2010

modeling gaseous pollutants and evaluating an advanced modeling system over East Asia, Atmos. Environ., 42, 3571–3583, 2008.
Geng, F. H., Tie, X., Xu, J. M., Zhou, G. Q., Peng, L., Gao, W., Tang, X., and Zhao, C. S.: Characterizations of ozone, NO_x, and VOCs measured in Shanghai, China, Atmos. Environ., 42, 6873–6883, 2008.
Huang, W., Tan, J., Kan, H. D., Zhao, N., Song, W. M., Song, G. X., Chen, G. H., Jiang, L. L., Jiang, C., Chen, R. J., and Chen, B. H.: Visibility, air quality and daily mortality in Shanghai, China, Sci. Total Environ., 407, 3295–3300, 2009.
Hu, M. C.: Environmental protection data manual, China Machine Press, Beijing, China, 1990 (in Chinese).
Jeffries, H. E.: Photochemical air pollution, in: Composition, Chemistry, and Climate of the Atmosphere, edited by: Singh, H. B., Van Nostrand-Reinhold, New York, USA, 1994.
Jiangsu Statistical Yearbook, China Statistics Press, Beijing, China, 2005.
Kato, N. and Akimoto, H.: Anthropogenic emissions of SO_2 and NO_x in Asia: emission inventories, Atmos. Environ., 26A, 2997–3017, 1992.
Kuang, J. X., Long, T., Huang, Q. F., and Jian, J. Y.: Study of emission factor for burning fuel, Environmental Monitoring in China, 17, 27–30, 2001 (in Chinese).
Lamb, R. G.: A regional-scale (1000 km) model of photochemical air pollution. Part I: theoretical formulation, US Environmental Protection Agency Report EPA/600/3-85-035, Research Triangle Park, NC, 1982.
Li, L., Chen, C. H., Huang, C., Huang, H. Y., Li, Z. P., Fu, J. S., Carey, J. J., and Streets, D. G.: Regional air pollution characteristics simulation of O_3 and PM_{10} over Yangtze River Delta Region, Environm. Sci., 29, 237–245, 2008 (in Chinese).
Lin, M., Holloway, T., Oki, T., Streets, D. G., and Richter, A.: Multi-scale model analysis of boundary layer ozone over East Asia, Atmos. Chem. Phys., 9, 3277–3301, doi:10.5194/acp-9-3277-2009, 2009.
Luo, C., St. John, J., Zhou, X., Lam, K., Wang, T., and Chameides, W.: A nonurban ozone air pollution episode over Eastern China: observations and model simulations, J. Geophys. Res., 105(D2), 1889–1908, 2000.
Ministry of Environmental Protection (MEP) of the People's Republic of China: User's Guide on the Production and Emission Factors of Industrial Pollutants, China Environmental Science Press, Beijing, China, 1996.
Pielke, R. A.: Mesoscale Meteorology Simulation, Meteorology Press, Beijing, China, 1990.

ACPD
10, 23657–23703, 2010

Shanghai Statistical Yearbook, China Statistics Press, Beijing, China, 2005.
Streets, D. G., Jiang, K., Hu, X., Sinton, J. E., Zhang, X.-Q., Xu, D., Jacobson, M. Z., and Hanson, J. E.: Recent reductions in China's greenhouse-gas emissions, Science, 294, 1835–1836, 2001.
Streets, D. G., Bond, T. C., Carmichael, G. R., Fernandes, S. D., Fu, Q., He, D., Klimont, Z., Nelson, S. M., Tsai, N. Y., Wang, M. Q., Woo, J.-H., and Yarber, K. F.: An inventory of gaseous and primary aerosol emissions in Asia in the year 2000, J. Geophys. Res., 108, 8809, doi:10.1029/2002JD003093, 2003a.
Streets, D. G., Yarber, K. F., Woo, J.-H., and Carmichael, G. R.: Biomass burning in Asia: annual and seasonal estimates and atmospheric emissions, Global Biogeochem. Cy., 17, 1099, doi:10.1029/2003GB002040, 2003b.
Streets, D. G., Fu, J. S., Jang, C. J., Hao, J., He, K., Tang, X., Zhang, Y., Wang, Z., Li, Z., Zhang, Q., Wang, L., Wang, B., and Yu, C.: Air quality during the 2008 Beijing Olympic Games, Atmos. Environ., 41, 480–492, 2007.
Streets, D. G. and Waldhoff, S. T.: Present and future emissions of air pollutants in China: SO_2, NO_x and CO, Atmos. Environ., 34, 363–374, 2000.
Tesche, T. W.: Photochemical dispersion modeling: review of model concepts and applications studies, Environ. Int., 9, 465–489, 1983.
United States Environmental Protection Agency: AP-42 Emission Factors, Washington, DC, 2006.
Uno, I., He, Y., Ohara, T., Yamaji, K., Kurokawa, J.-I., Katayama, M., Wang, Z., Noguchi, K., Hayashida, S., Richter, A., and Burrows, J. P.: Systematic analysis of interannual and seasonal variations of model-simulated tropospheric NO_2 in Asia and comparison with GOME-satellite data, Atmos. Chem. Phys., 7, 1671–1681, doi:10.5194/acp-7-1671-2007, 2007.
Wang, H. X., Tang, X. Y., Wang, M. L., Yan, P., Wang, T., Shao, K. S., Zeng, L. M., Du, H. F., and Chen, L. M.: The temporal and spatial allocation characteristics of trace gases in the Yangtze River Delta, Sci. China (Series D), 33, 114–118, 2003 (in Chinese).
Wang, T., Cheung, V. T. F., Anson, M., and Li, Y. S.: Ozone and related gaseous pollutants in the boundary layer of Eastern China: overview of the recent measurements at a rural site, Geophys. Res. Lett., 28, 2373–2376, 2001a.
Wang, T., Wei, X. L., Ding, A. J., Poon, C. N., Lam, K. S., Li, Y. S., Chan, L. Y., and Anson, M.: Increasing surface ozone concentrations in the background atmosphere of Southern China, 1994–2007, Atmos. Chem. Phys., 9, 6217–6227, doi:10.5194/acp-9-6217-2009, 2009.

ACPD
10, 23657–23703, 2010

Wang, X., Zhang, Y., Hu, Y., Zhou, W., Lu, K., Zhong, L., Zeng, L., Shao, M., Hu, M., and Russell, A. G.: Process analysis and sensitivity study of regional ozone formation over the Pearl River Delta, China, during the PRIDE-PRD2004 campaign using the Community Multiscale Air Quality modeling system, Atmos. Chem. Phys., 10, 4423–4437, doi:10.5194/acp-10-4423-2010, 2010.

Wang, X. M., Fu, C., and Liang, G. X.: Study on the ozone concentration in urban areas, Res. Environm. Sci., 14, 1–3, 2001b.

Wang, Y., Zhuang, G. S., Zhang, X. Y., Huang, K., Xu, C., Tang, A. H., Chen, J. M., and An, Z. S.: The ion chemistry, seasonal cycle, and sources of $PM_{2.5}$ and TSP aerosol in Shanghai, Atmos. Environ., 40, 2935–2952, 2006.

Xu, J., Zhu, Y., and Li. J.: Case studies on the processes of surface ozone pollution in Shanghai, J. Air Waste Manage., 49, 716–724, 1999.

Ye, B. M., Ji, X. L., Yang, H. Z., Yao, X. H., Chan, C. K., Cadle, S. H., Chan, T., and Mulawa, P. A.: Concentration and chemical composition of $PM_{2.5}$ in Shanghai for a 1-year period, Atmos. Environ, 37, 499–510, 2003.

Zhang, M. G., Uno, I., Yoshida, Y., Xu, Y. F., Wang, Z. F., Akimoto, H., Bates, T., Quinn, T., Bandy, A., and Blomquist, B.: Transport and transformation of sulfur compounds over East Asia during the TRACE-P and ACE-Asia campaigns, Atmos. Environ., 38, 6947–6959, 2004.

Zhang, M. G.: Numerical simulation with a comprehensive chemical transport model of nitrate, sulfate, and ammonium aerosol distributions over East Asia, China Part., 3, 255–259, 2005.

Zhang, M. G., Han, Z. W., and Zhu, L. Y.: Simulation of atmospheric aerosols in East Asia using modeling system RAMS-CMAQ: model evaluation, China Part., 5, 321–327, 2007.

Zhejiang Statistical Yearbook, China Statistics Press, Beijing, China, 2005.

Zhu, Y. X. and Xu, J. L.: Ozone pollution process in the lower atmosphere and the meteorological factors concerned, Res. Environ. Sci., 7, 13–18, 1994 (in Chinese).

ACPD

10, 23657–23703, 2010

Table 1. Residential fuel consumption in the YRD in 2004.

Province or municipality	City	Population (millions)	Coal (10^4 t)	LPG (10^4 t)	Coal gas (10^6 m^3)	Nat gas (10^6 m^3)
Jiangsu Province	Nanjing	5.8	7.0	9.8	76.9	3.1
	Wuxi	4.5	5.6	3.7	29.2	1.2
	Changzhou	3.5	4.3	4.9	38.0	1.5
	Suzhou	6.0	7.4	7.1	55.4	2.3
	Nantong	7.7	9.7	5.6	44.2	1.8
	Yangzhou	4.5	5.8	1.5	11.4	0.5
	Zhenjiang	2.7	3.3	3.6	28.2	1.1
	Taizhou	5.0	6.2	5.2	40.8	1.7
	Total	**39.8**	**49.3**	**41.4**	**324.1**	**13.2**
Zhejiang Province	Hangzhou	6.5	8.6	23.0	12.7	0.0
	Ningbo	5.5	6.6	16.2	7.9	0.0
	Jiaxing	3.3	4.0	9.9	4.9	0.0
	Huzhou	2.6	3.0	7.2	3.4	0.0
	Shaoxing	4.3	5.0	11.8	5.4	0.0
	Zhoushan	1.0	1.2	3.0	1.6	0.0
	Taizhou	5.6	5.9	12.0	4.3	0.0
	Total	**28.8**	**34.4**	**83.0**	**40.3**	**0.0**
Shanghai Municipality		**13.5**	**80.6**	**20.4**	**1223.0**	**197.0**
Regional Total		**82.1**	**164.3**	**144.8**	**1587.4**	**210.2**

ACPD
10, 23657–23703, 2010

Table 2. MM5 model performance assessment.

Time	Value	Coefficient	σ/σ_{obs}	E/σ_{obs}	E_{UB}/σ_{obs}
1 Jan 2004, 20:00 LT	*U*	0.9154	0.8809	0.7084	0.4039
	V	0.9227	0.9104	0.5331	0.3858
2 Jan 2004, 08:00 LT	*U*	0.9547	1.2017	0.7834	0.3866
	V	0.9464	0.6692	0.4257	0.4257
20 Jan 2004, 08:00 LT	*U*	0.8572	1.2097	1.6466	0.6241
	V	0.8220	0.6985	0.5969	0.5827
25 Jan 2004, 08:00 LT	*U*	0.8608	1.0367	1.4298	0.5396
	V	0.8887	0.7201	0.5238	0.4885
28 Jan 2004, 08:00 LT	*U*	0.8972	0.9431	0.7717	0.4441
	V	0.9581	0.9281	0.4556	0.2878
1 Jul 2004, 20:00 LT	*U*	0.8523	1.3554	0.9256	0.7257
	V	0.9054	0.8832	0.4828	0.4251
2 Jul 2004, 08:00 LT	*U*	0.7900	0.2832	0.8148	0.7869
	V	0.5923	1.4745	1.1973	1.1948

ACPD
10, 23657–23703, 2010

Table 3. Statistical comparison of the CMAQ predicted values with the observational data.

Month	January						July					
Pollutants	SO_2 ($mg\,m^{-3}$)		NO_2 ($mg\,m^{-3}$)		PM_{10} ($mg\,m^{-3}$)		SO_2 ($mg\,m^{-3}$)		NO_2 ($mg\,m^{-3}$)		PM_{10} ($mg\,m^{-3}$)	
Item	Obs	Model	Obs	Model	Obs	Model	Obs	Model	Obs	Model	Obs	Model
Hourly Average	0.045	0.052	0.043	0.05	0.083	0.041	0.036	0.039	0.033	0.038	0.017	0.018
Max.	0.19	0.337	0.121	0.119	0.274	0.109	0.181	0.297	0.11	0.111	0.050	0.057
Min.	0.004	0.001	0.007	0.007	0.000	0.000	0.005	0.003	0.005	0.002	0.000	0.000
R^2 correlation coefficient	0.51		0.66		0.4		0.69		0.64		0.52	
Index of agreement	0.55		0.79		0.45		0.79		0.75		0.53	
Bias	25%		29%		–24%		13%		22%		26%	
Factor of two	59%		80%		51%		75%		81%		73%	
Number of data points	960		960		480		1200		1200		480	

ACPD
10, 23657–23703, 2010

Table 4. Deciview values and corresponding visibility levels.

Dcv	Visibility level
≤14	Very good
15–20	Good
21–24	Moderate
25–28	Bad
≥29	Very bad

ACPD
10, 23657–23703, 2010

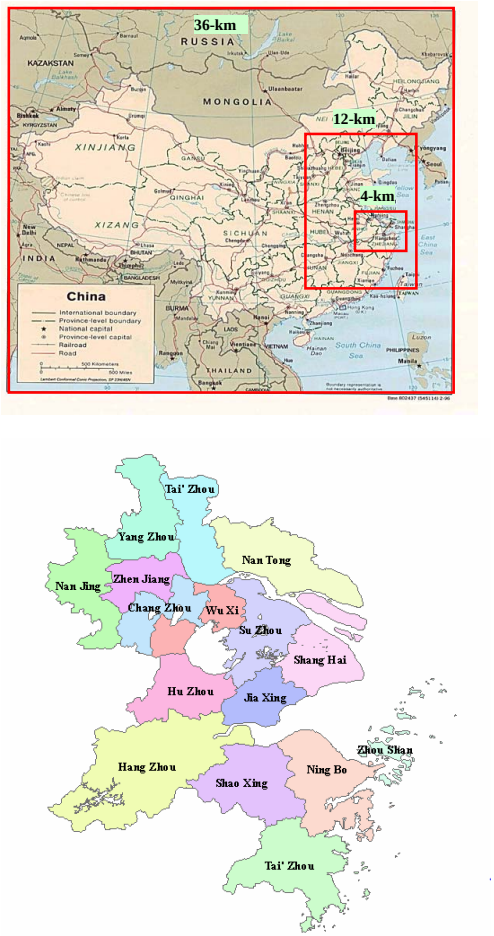

Fig. 1. Three-way nested model domain (top) and locations of the 16 cities in the YRD (bottom).

ACPD
10, 23657–23703, 2010

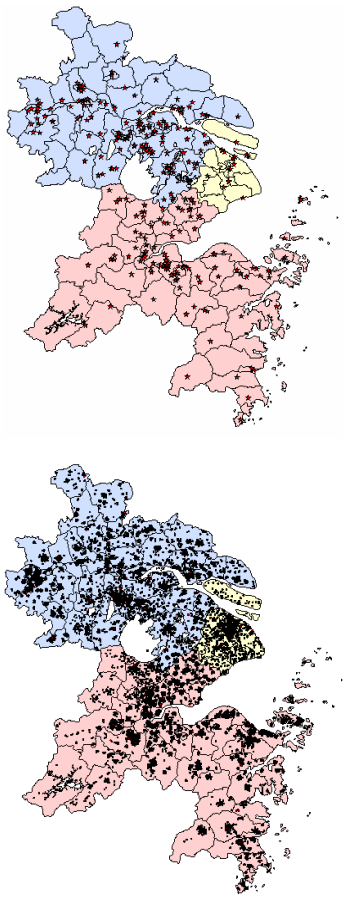

Fig. 2. Distribution of point sources in the YRD (top: power plants; bottom: industrial point sources); Jiangsu Province is shown in blue, Zhejiang Province in pink, and the Shanghai Municipality in yellow.

ACPD
10, 23657–23703, 2010

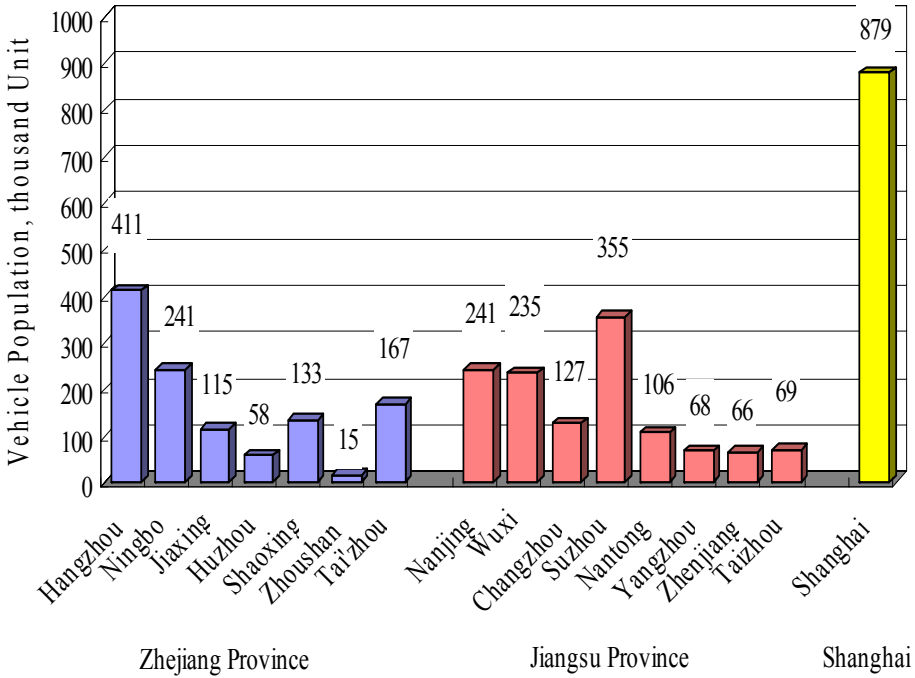

Fig. 3. Vehicle stocks (without motorcycles) of the 16 major cities of the YRD in 2004.

ACPD
10, 23657–23703, 2010

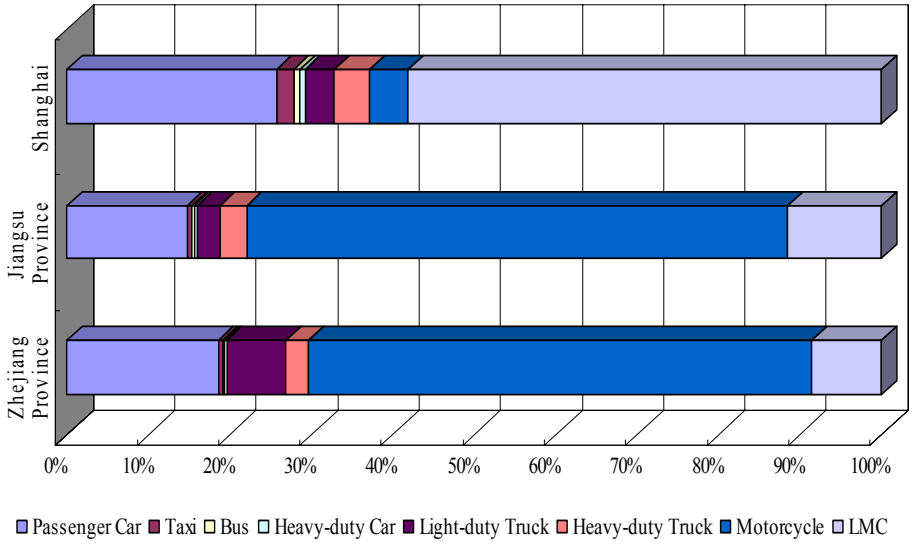

Fig. 4. Vehicle categories in the two provinces and Shanghai in 2004.

ACPD
10, 23657–23703, 2010

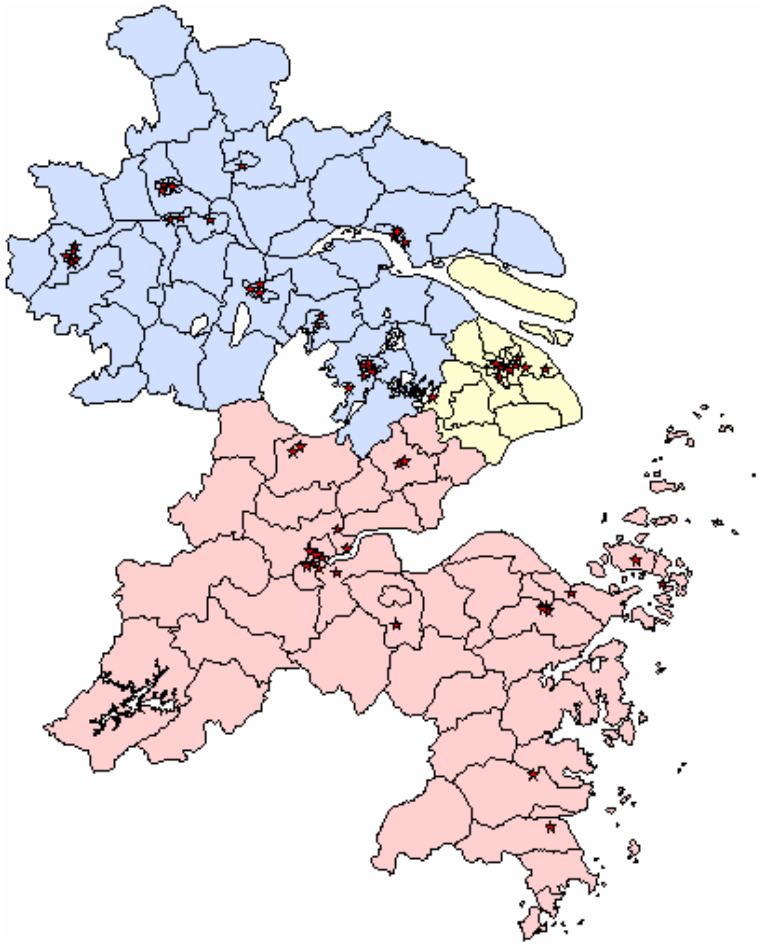

Fig. 5. Locations of the national observational sites used in the model performance assessment.

ACPD
10, 23657–23703, 2010

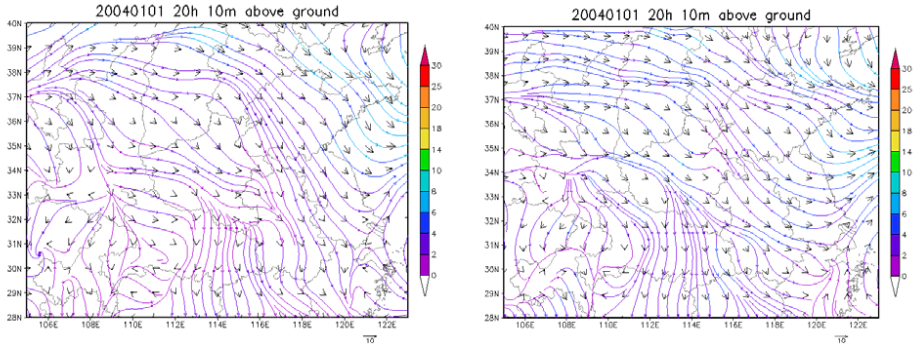

Fig. 6. Subjective test of MM5 performance for 1 January 2004, 20:00 LT: NCEP observational data (left); MM5 model result (right).

ACPD
10, 23657–23703, 2010

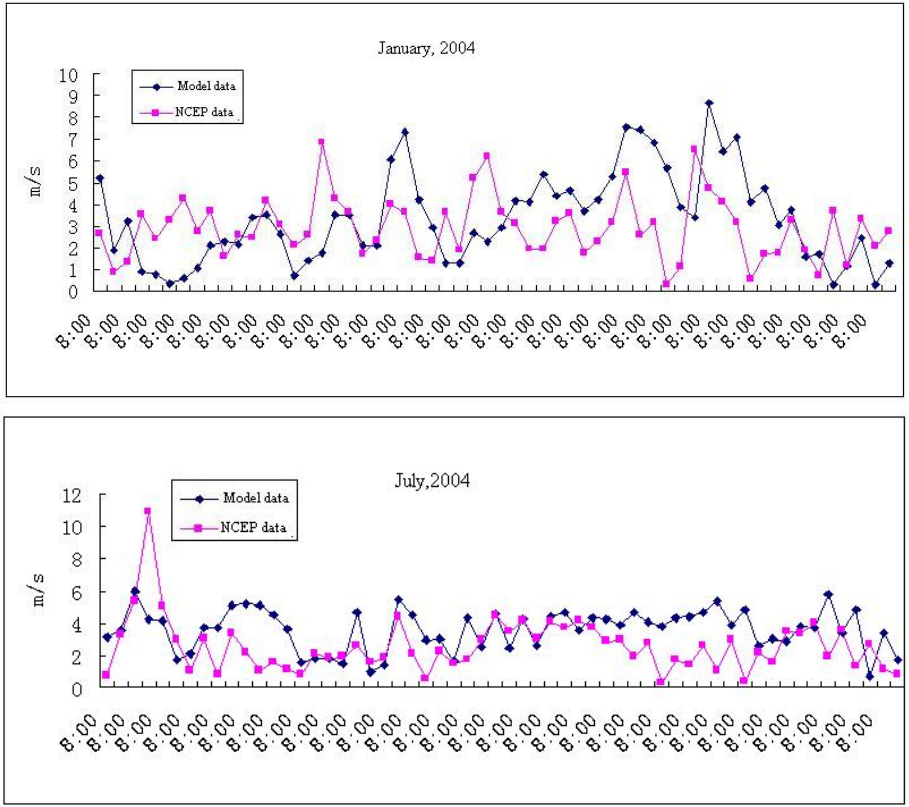

Fig. 7. Wind speed comparison between NCEP and model data for January and July, 2004.

ACPD
10, 23657–23703, 2010

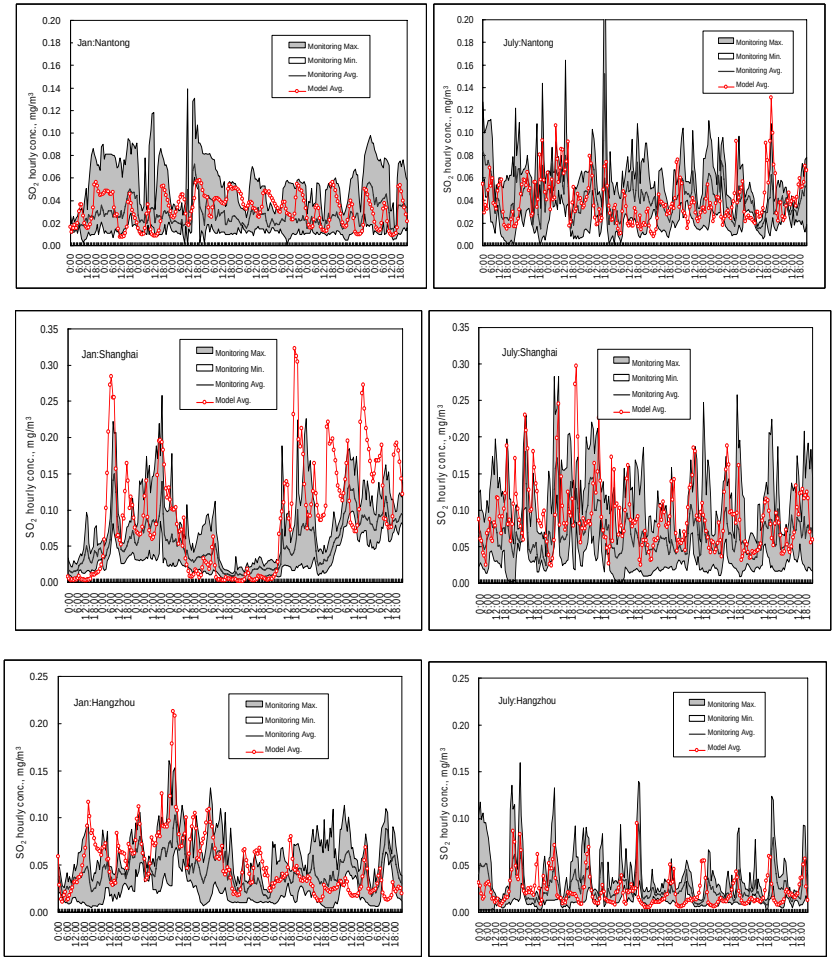

Fig. 8. Comparison of CMAQ model simulations for SO_2 concentrations against observations.

ACPD
10, 23657–23703, 2010

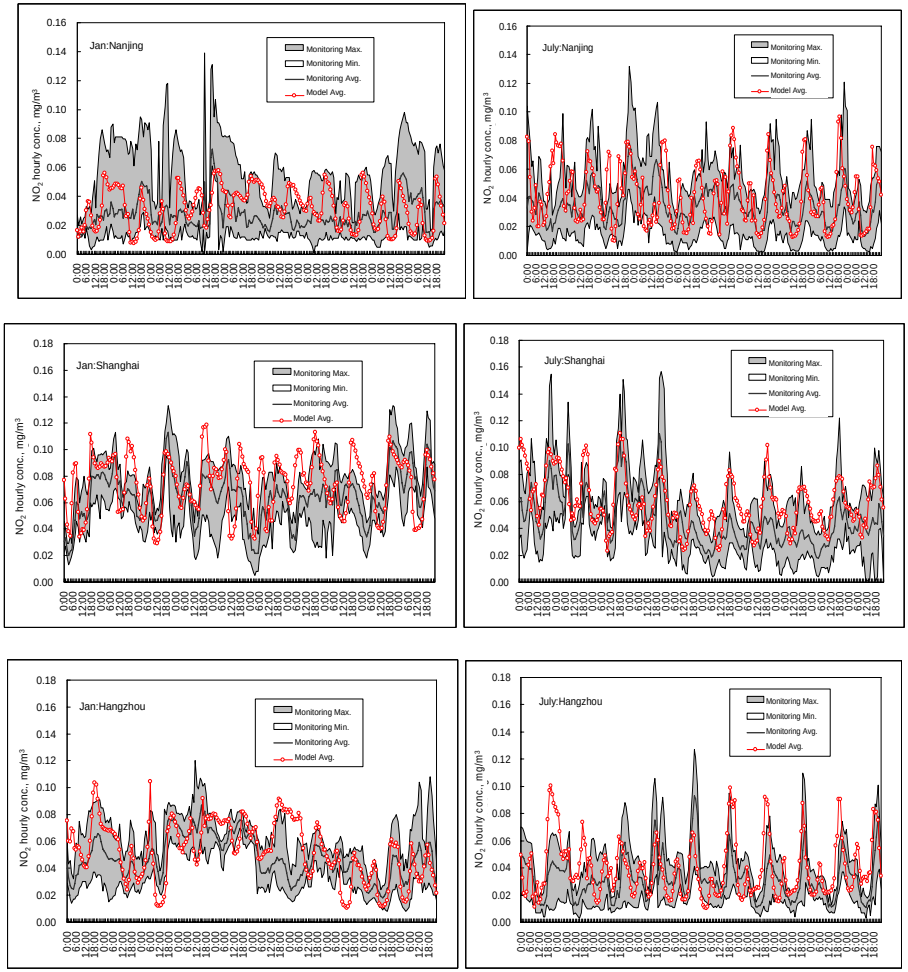

Fig. 9. Comparison of CMAQ model simulations for NO_2 concentrations against observations.

ACPD
10, 23657–23703, 2010

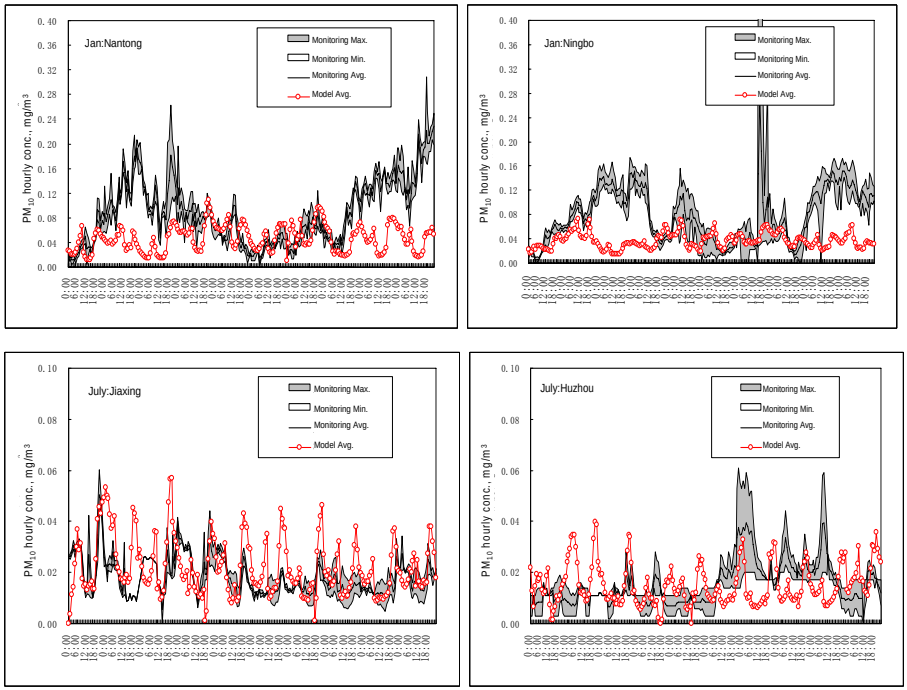

Fig. 10. Comparison of CMAQ model simulations for PM_{10} concentrations against observations.

ACPD
10, 23657–23703, 2010

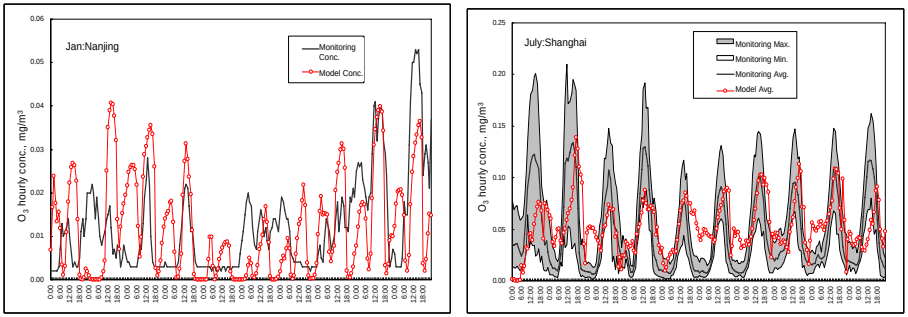

Fig. 11. Comparison of CMAQ model simulations for O_3 concentrations against observations.

ACPD
10, 23657–23703, 2010

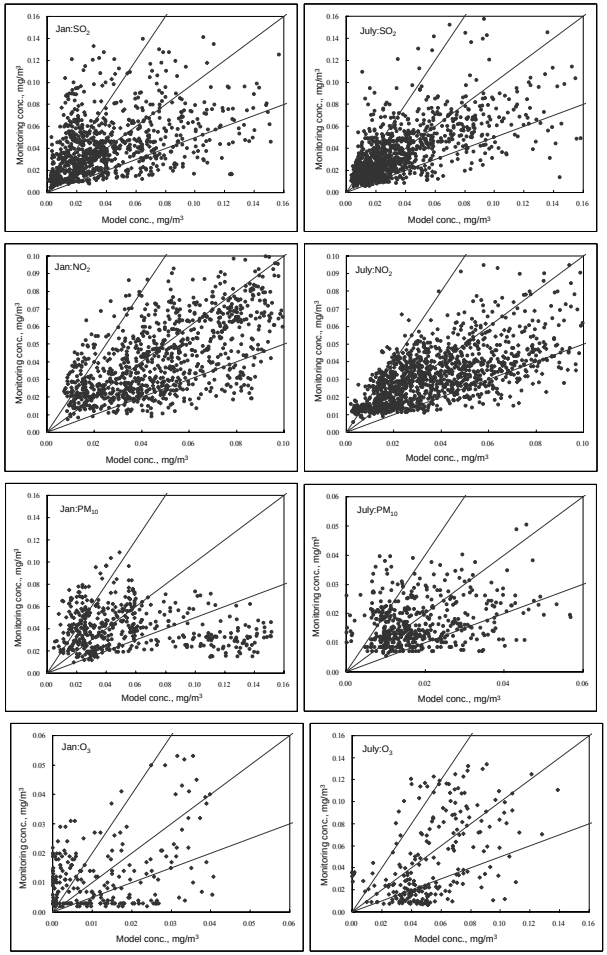

Fig. 12. Factor 2 analyses of model results (January and July) for SO_2, NO_2, PM_{10}, and O_3.

ACPD
10, 23657–23703, 2010

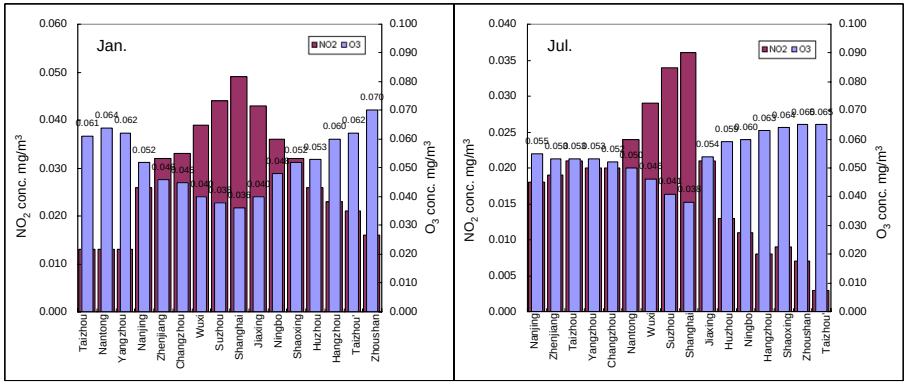

Fig. 13. Monthly average concentrations of O_3 among the 16 cities in the YRD.

ACPD
10, 23657–23703, 2010

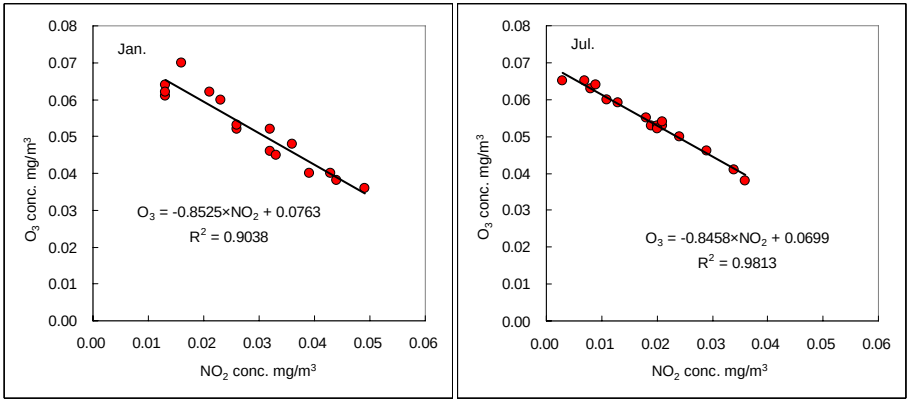

Fig. 14. Relationship between monthly average concentrations of O_3 and NO_2 in 16 cities in the YRD.

ACPD
10, 23657–23703, 2010

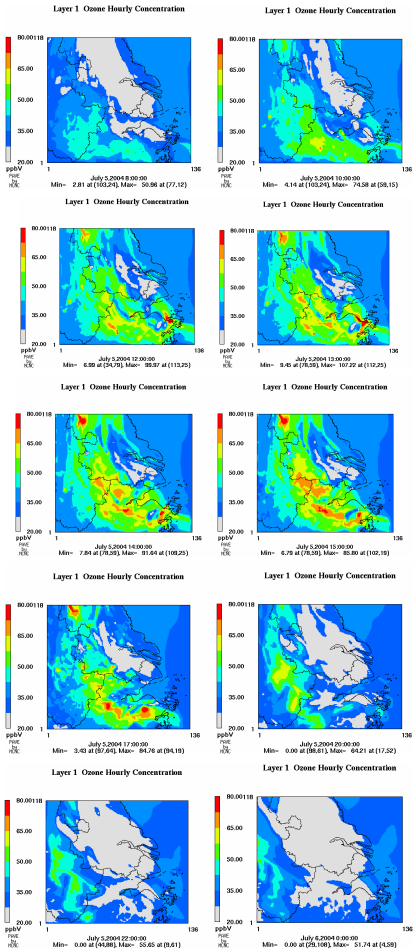

Fig. 15. Spatial distributions of hourly O_3 concentrations on 5 July 2004.

ACPD
10, 23657–23703, 2010

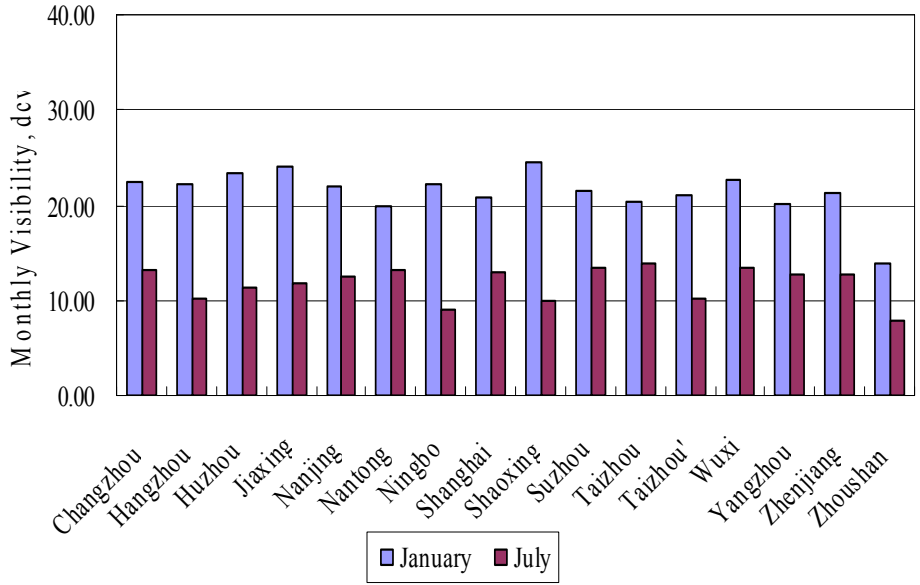

Fig. 16. Visibility, measured as deciview (dcv), in the 16 cities of the YRD.

ACPD
10, 23657–23703, 2010

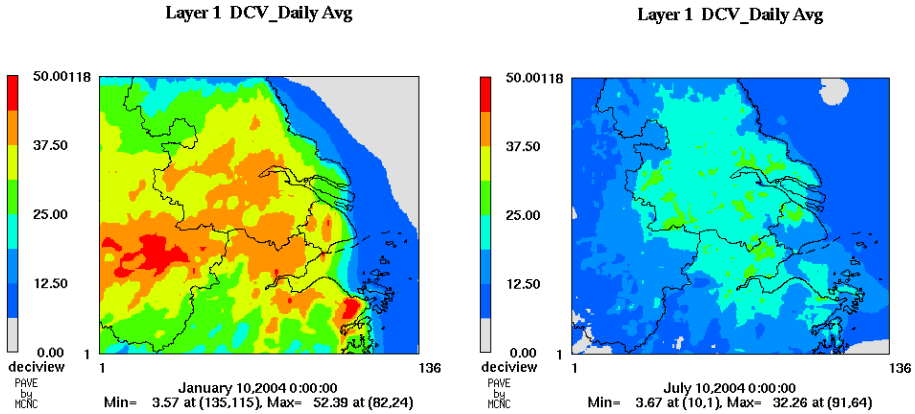

Fig. 17. Modeled visibility in the YRD.

ACPD
10, 23657–23703, 2010

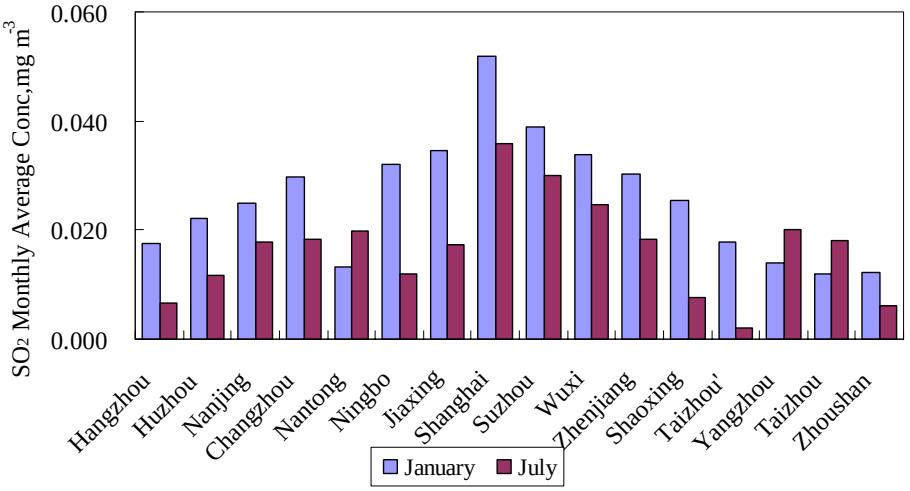

Fig. 18. Monthly average concentrations of SO_2 in the 16 cities of the YRD.

ACPD
10, 23657–23703, 2010

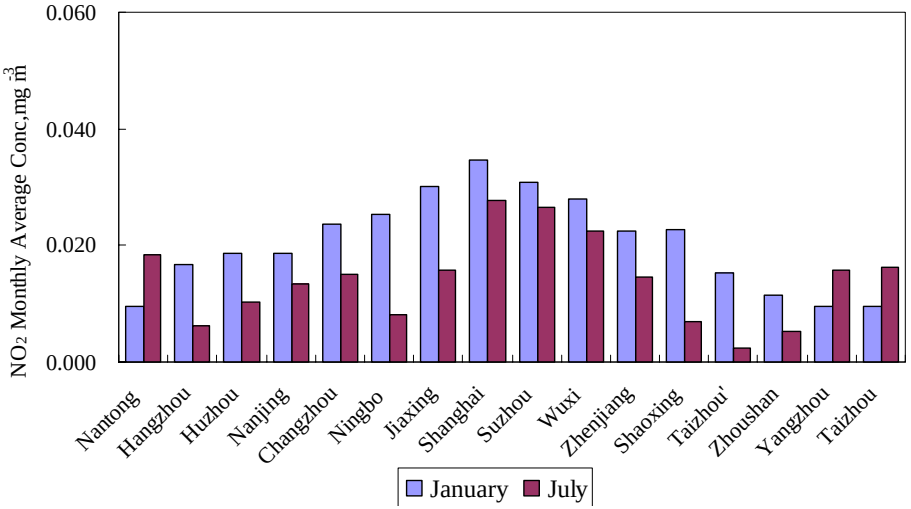

Fig. 19. Monthly average concentrations of NO_2 in the 16 cities of the YRD.

ACPD
10, 23657–23703, 2010